

Identification of Biomarkers with Therapeutic And prognostic Value in Skin Cutaneous Melanoma

Guangwen Wang

Maoming People's Hospital

Yonghuo Ling

Maoming People's Hospital

Qianru Zhuang

Maoming People's Hospital

Yingbang Li

Maoming People's Hospital

Yunpeng Bai

Maoming People's Hospital

Yisheng Huang

Maoming People's Hospital

Wendong Huang (✉ huangwendong418@126.com)

Maoming People's Hospital <https://orcid.org/0000-0002-6119-5847>

Primary research

Keywords: Skin cutaneous melanoma (SKCM), TCGA, Tumor microenvironment, Biomarker

Posted Date: July 1st, 2020

DOI: <https://doi.org/10.21203/rs.3.rs-38604/v1>

License:  This work is licensed under a Creative Commons Attribution 4.0 International License.

[Read Full License](#)

Abstract

Background

The morbidity and mortality of skin cutaneous melanoma (SKCM), the most deadly type of skin cancer, are on the rise worldwide. Through in-depth study of the tumor microenvironment (TME) of SKCM, this study further identified biomarkers with therapeutic and prognostic value.

Methods

The gene expression profiles and clinical data of SKCM patients were downloaded from The Cancer Genome Atlas database. Then we calculated the immune score and stromal score of patients with skin melanoma by using the estimate algorithm, and divided all patients into the high/low immune/stromal score groups and discussed the correlation between them and clinical characteristics. Then, limma R package was used to screen out the differential genes in the high/low immune/ stromal score groups, and the heat map of the differential genes was drawn. At the same time, the functional enrichment analysis of the differential genes was carried out. The protein–protein interaction (PPI) network of different genes was constructed by using STRING and Cytoscape, and the key genes related to the prognosis of cutaneous melanoma were further selected. Finally, kinase target, co expression genes and immune infiltrating cells of key genes were discussed.

Results

Patients in the low-immune/stromal score group had poorer survival outcome. The immune and stromal scores are associated with specific clinicopathologic variables (age, tumor grade, tumor stage) in SKCM. In total, 914 DEGs (909 upregulated and 5 downregulated genes) were screened from the gene expression profiles of patients with high immune and stromal scores. Functional enrichment analysis demonstrated a correlation between DEGs and the tumor microenvironment, tumor immune response and RCC tumorigenesis. Kaplan-Meier survival curves showed that 15 out of the 914 identified tumor microenvironment related genes are involved in the prognosis of SKCM. Finally *CXCR8* and *CCR5* were selected as the hub genes. A positive correlation was obtained between the expression of *CXCR8/CCR5* and the abundance of six immune cells.

Conclusions

We studied the tumor microenvironment of SKCM, and finally screened out the biomarkers with therapeutic and prognostic effects.

1. Background

Although skin cutaneous melanoma (SKCM) accounts for only 2% of all skin cancers[1], it is the most deadly type of skin cancer because of its high degree of malignancy and invasiveness. Indeed, the higher the SKCM stage, the higher the 5-year mortality. The I–IV survival rates were 97% (IA), 84% (IB), 68% (II), 55% (III), and 17% (IV)[2]. While continuous progress and medical technological innovations have prolonged the survival of patients and decreased mortality rates, the incidence of malignant SKCM continues to increase annually at an alarming rate[3]. Previous reports indicated that early diagnosis and accurate prognosis of patients with SKCM are very important for formulating optimal treatment plans and improving quality of life. However, no clinical biomarker that can accurately predict the prognosis of patients with SKCM is yet available. Thus, exploring the biomarker of SKCM is necessary to improve the treatment and prognosis of patients.

The tumor microenvironment (TME), which refers to the tumor cell environment composed of extracellular stromal molecules, inflammatory mediators, and various cells (e.g., immune cells, interstitial cells, and endothelial cells)[4, 5], plays an important role in SKCM tumor metastasis, cell proliferation, invasion, and other biological behaviors[6]. Immune and stromal cells, as important non-tumor components of the TME, participate in tumor information transmission, immune monitoring, and niche formation. Previous studies demonstrated the diagnostic and prognostic value of immune and stromal cells in tumors[7, 8]. This algorithm is based on gene expression features and can reflect the proportion of stromal and immune cells in tumor tissues to evaluate tumor purity[9]. An increasing number of researchers have used this algorithm to study different tumor types, such as glioblastoma[5], breast cancer[10], prostate cancer[11], and colon cancer[12]. However, applying ESTIMATE algorithm is necessary to explore the function of stromal and immune cells in SKCM.

In this study, the RNA expression profiles and clinical data (age, sex, tumor stage, survival status and prognosis) of patients with SKCM were extracted from The Cancer Genome Atlas (TCGA) database, which was established by the U.S. government to identify and catalog oncogene changes[13]. We then used the ESTIMATE algorithm[9] and tumor immune evaluation resource (TIMER)[14] to analyze the immune cells and genes in the SKCM TME. We not only studied the correlation between immune/stromal scores and clinical symptoms but also examined the relationship between TME-related genes and the prognosis of patients with SKCM. Finally, we identified the hub genes of SKCM and identified their kinase targets, co-expressed genes, and correlations with immune cell infiltration. Our results show that the composition of the TME affects the clinical prognosis of patients with SKCM. This finding may provide a basis for the future development of new prognostic biomarkers and treatment methods, especially immunotherapy.

2. Materials And Methods

2.1. Gene expression datasets

The gene expression profiles (level 3 data) of skin cutaneous melanoma patients were extracted from the TCGA database (<https://tcga-data.nci.nih.gov/tcga/>). The RNA expression patterns of SKCM patients

were analyzed using the Illumina HiSeq. Then the clinical data of SKCM patients were extracted, including gender, age, grade, stage and survival status. After downloading and transposing the data, immune and stromal scores were calculated by performing the ESTIMATE algorithm .

2.2. Survival rates of immune/gene scores and their association with clinical characteristics

According to the ESTIMATE algorithm results, all samples were divided into high/low immune score groups and high/low stromal score groups to select crossover genes. Kaplan-Meier method was used to assess the prognostic value of the scores in skin cutaneous melanoma, and the overall survival curve was generated by R software. In addition, we studied the correlation between immune/stromal scores and clinical characteristics.

2.3. Identification of differentially expressed genes

Evidence of differential gene expression was analyzed using the “limma” package. Differentially expressed genes (DEGs) were screened by $|\log_2FC| > 2$ and $adj.P < 0.05$. Clustering analysis and the construction of immune and stromal heatmaps were done using the pheatmap R package .

2.4. Enrichment analysis of DEGs

Functional annotation of DEGs was carried out by means of gene ontology (GO) analysis and Kyoto encyclopedia of genes and genomes (KEGG). Go analysis is primarily used to study cellular composition (CC), molecular function (MF), and biological processes (BP). GO and KEGG pathway analyses results were processed by the “clusterProfiler”, “enrichplot”, and “ggplot2” packages. The P-value and q-value cut-offs were set at 0.05 each.

2.5. Construction of PPI network

Protein-protein interaction (PPI) networks can be generated using the STRING database[15]. The required minimum interaction score was set at 0.4. In addition, we used CytoHubba plug-in in Cytoscape to detect each module of PPI network and explore the key genes.

2.6. Overall survival curve of all DEGs

The prognostic value of DEGs in SKCM was evaluated using the Kaplan-Meier method, and overall survival curves were generated by the R software. The log-rank test was used to assess the prognostic value of the identified DEGs.

2.7. LinkedOmics

The Linkedomics (<http://www.links.org/>) database is a platform for accessing, analyzing, and comparing internal recombination data for different tumor types[16]. In this study, the LinkInterpreter module of LinkedOmics was used to explore the kinase target of SKCM hub genes. At the same time, the coexpression of key genes was also studied.

2.8. TIMER

The TIMER (<https://cistrome.shinyapps.io/timer/>) database is a practical platform for the systematical analysis of immune infiltrates in diverse cancer types. The current study used the TIMER Gene module to explore the correlation between the abundances of six immune in-filtrates and the level of hub genes.

3. Results

3.1. Patient characteristics

In February 2020, the gene expression profiles and relevant clinicopathological variables of 471 patients with SKCM were extracted from the TCGA database. Among these patients, 293 were male (62.21%) and 178 were female (37.79%). The median age of the included cases was 58 years (range, 15–90 years). In this study, the numbers of patients with tumor grades G1, G2, G3, and G4 were 5 (1.1%), 18 (3.8%), 77 (16.3%), and 167 (35.5%), respectively. In total, 78 cases were diagnosed with stage I SKCM (16.6%), 141 were diagnosed with stage II SKCM (29.9%), 175 were diagnosed with stage III SKCM (37.2), and 23 were diagnosed with stage IV SKCM (4.9%). The most common tumors were in T4 group (33.1%, n = 156); T1, T2 and T3 groups were 8.9% (n = 42), 16.3% (n = 77) and 20.0% (n = 94), respectively. In addition, 184 patients had regional lymph node metastasis while 24 had distant metastasis.

3.2. Correlation between immune/stromal scores and clinicopathologic variables of skin cutaneous melanoma

In this study, complete gene expression profiles and clinicopathological information from the TCGA database were used to analyze the data of all cases. According to the data of the ESTIMATE algorithm, stromal scores ranged from -1806.74 to 1892.23, immune scores ranged from -1481.02 to 3769.31, and ESTIMATE scores ranged from -2632.50 to 5077.47. The mean immune ($P=0.009$), stromal ($P=0.012$), and ESTIMATE ($P=0.006$) scores of patients with SKCM in the older-age group were consistently lower than those of patients in the lower-age group (Fig. 1A). Moreover, the mean immune ($P=1.78e-04$), stromal ($P=3.69e-03$), and ESTIMATE ($P=3.95e-04$) scores differed among stages I, II, III, and IV (Fig. 1B); here, the overall trend showing an initial decrease followed by a gradual increase. The mean immune ($P=5.14e-04$), stromal ($P=0.017$), and ESTIMATE ($P=1.83e-03$) scores also varied according to tumor stage (Fig. 1C). These results suggest that stromal, immune, and assessment scores are correlated with certain clinicopathologic variables.

Kaplan–Meier survival curves were drawn to assess the potential associations between overall survival and immune, stromal, and assessment scores. First, the 471 patients with SKCM were divided into high and low groups according to their scores. Immune score results showed that, compared with the high-score group, the overall survival time of patients with SKCM in the low-score group was longer (Fig. 2A, $P=0.001$). ESTIMATE score results showed that the overall survival time of patients with SKCM in the low-score group was longer than that in the high-score group (Fig. 2, $P=0.001$). Finally, stromal scores (Fig.

2B, $P=0.069$) indicated that the overall survival time of patients in the low-score group was longer than that in the high-score group, but the difference was not statistically significant.

Next, we analyzed Affymetrix chip data from our 471 patients to reveal differences in gene expression profiles based on immune and stromal scores. A heat map drawn on the basis of immune scores is shown in Fig. 3A, which showed 1049 and 94 up-regulated genes in the high- and low-score groups, respectively ($|\text{fold change}|>2$, $P<0.05$). Fig. 3B shows the heatmaps drawn on the basis of stromal scores; here, 1369 and 30 genes were up-regulated in the high- and low-score groups, respectively ($|\text{fold change}|>2$, $P<0.05$). Differentially expressed genes (DEGs) in the immune and stromal score groups were identified by Venn map. Our results showed that 909 genes were up-regulated in the high-score group (Fig. 4A) while 5 genes were down-regulated in the low-score group (Fig. 4B).

3.3. Functional enrichment analysis of differentially expressed genes

Gene Ontology (GO) and Kyoto Encyclopedia of Genes and Genomes (KEGG) were used for functional enrichment analysis to determine the functions of DEGs. GO analysis was employed to determine the top 10 biological processes (BP), top 10 molecular functions (MF), and top 10 cellular components (CC) (Fig. 5A). The top 10 enriched BPs included leukocyte cell–cell adhesion, T-cell activation, T-cell aggregation, lymphocyte aggregation, leukocyte aggregation, adaptive immune response, regulation of leukocyte activation, and regulation of lymphocyte activation. These BPs are involved in the tumor immune response. The top 10 enriched MFs included cytokine activity, cytokine receptor activity, chemokine activity, cytokine receptor binding, chemokine receptor binding, CCR chemokine receptor binding, antigen binding, carbohydrate binding, G-protein coupled chemoattractant receptor activity, and chemokine receptor activity. These MFs are also associated with the tumor immune response. The top 10 CCs included side of membrane, external side of plasma, MHC class II protein complex, T-cell receptor complex, MHC protein complex, receptor complex, immunological synapse and plasma membrane receptor Integral component of luminal side of endoplasmic reticulum. KEGG analysis yielded similar results (Fig. 5A). KEGG pathway analysis also indicated that the cytokine–cytokine receptor interaction and chemokine signaling pathways are involved in the tumor immune response and SKCM development.

The STRING tool was used to explore the protein–protein interaction (PPI) network and elucidate interactions between DEGs. The functional network consisted of 14 modules, 339 nodes and 848 edges (Fig. 6A). The first 20 significant genes were *CCR2*, *CD8B*, *CXCL11*, *CXCL13*, *CXCR3*, *CD72*, *CCL25*, *CD3G*, *C1R*, *C1S*, *CXCL9*, *CCL21*, *CCR7*, *CXCR5*, *CCR8*, *CXCL16*, *CXCL10*, *C1QC*, *HLA-DRB5* and *CCL19* (Fig. 6B).

3.4. Role of individual DEGs in overall survival in skin cutaneous melanoma

In this study, Kaplan–Meier survival curves were drawn to determine the potential function of 909 up-regulated and 5 down-regulated genes in the overall survival of SKCM patients. The log-rank test showed that, among 1014 DEGs, *AQP9*, *CCR8*, *PATL2*, *RGL4*, *OR9G1*, *CXCR5*, *IPCEF1*, *FCRL3*, *RCSD1*, *CP*, *NEXN*, *MAFB*, *SLC40A1*, and *TNFRSF13B* have significant predictive effects on the overall survival of SKCM (Fig. 7, all $P<0.05$).

3.5. Identification of the kinase target of hub genes

Among the top 20 important genes (i.e., *CD72*, *CXCR5*, *CCR8*, *CXCL13*, *CXCR3*, *CXCL16*, *CXCL10*, *CCR2*, *CD8B*, *CXCL11*, *CCL25*, *CD3G*, *C1R*, *C1S*, *CXCL9*, *CCL21*, *CCR7*, *C1QC*, *HLA-DRB5*, and *CCL19*) found in the PPI network, *CCR8* and *CXCR5* were significantly correlated with the overall survival of SKCM patients. Therefore, these DEGs were selected as hub genes. We explored the kinase targets of these genes by using the LinkedOmics database and found that *PRKCA*, *ATM*, *PLK1*, *CHEK1*, and *ATR* are the five most significant kinase target networks for *CXCR5*. Moreover, kinases *LYN*, *FYN*, *AURKB*, *PAK1*, and *LCK* were the five most prominent target networks for *CCR8* (Table 1). We also studied the co-expression genes of *CXCR5*(Fig. 8A) and *CCR8* (Fig. 8B).

3.6. Immune landscape of the tumor microenvironment in melanoma

We analyzed the correlation between hub genes and immune cell infiltration. Our results revealed a positive correlation between *CCR8* expression and CD8+ T cells (Cor=0.592, P=8.51e-43), CD4+ T cells (Cor=0.389, P=1.34e-17), B-cell infiltration (Cor=0.327, P= 1.17e-12), macrophages (Cor=0.412, P=5.83e-20), neutrophils (Cor=0.662, P=2.27e-58), and dendritic cells (Cor=0.625, P=1.33e-49) (Fig. 9A). Similar results were also obtained for *CXCR5*. Specifically, *CXCR5* expression was positively correlated with CD8+ T cells (Cor=0.413, P=1.63e-19), CD4+ T cells (Cor=0.49, P=2.48e-28), B-cell infiltration (Cor=0.419, P=1.75e-20), macrophages (Cor=0.223, P=1.62e-06), neutrophils (Cor=0.398, P=1.21e-18), and dendritic cells (Cor=0.488, P=4.02e-28) (Fig. 9B).

4. Discussion

SKCM is one of the most deadly skin diseases worldwide. Although the overall survival of patients with SKCM has improved, mortality remains high mainly because the prognosis and therapeutic biomarkers of the disease have not been identified. In this study, SKCM data were extracted from the TCGA database to investigate the TME genes affecting the overall survival and tumorigenesis of SKCM. We then identified potential biomarkers for the prognosis and treatment of this lethal form of melanoma.

We used the ESTIMATE algorithm to obtain immune and stromal scores to understand the TME of SKCM. The relationship between the clinicopathological variables of SKCM and immune and stromal scores was then evaluated. Our results showed that immune and stromal scores were correlated with specific clinicopathologic variables, namely, age, tumor stage, and T stage. In addition, the immune and stromal scores could predict the prognosis of patients with SKCM accurately. We divided the samples into high- and low-immune/stromal score groups to understand the correlation between TME and survival rate. Our results suggest that patients with SKCM and low-immune, stromal, and ESTIMATE scores have longer overall survival times than those with high scores.

We identified 914 DEGs after comparing the high- and low-immune/stromal score groups. GO and KEGG pathway analysis revealed that many DEGs are involved in the tumor immune response, tumorigenesis, and TME maintenance. For example, GO analysis showed that DEGs are enriched in leukocyte cell-cell

leukocytes, T-cell activation, T-cell aggregation, lymphocyte aggregation, leukocyte aggregation, adaptive immune response, regulation of leukocyte activation, regulation of lymphocyte activation, cytokine activity, cytokine receptor activity, chemokine activity, cytokine receptor binding, chemokine receptor binding, CCR chemokine receptor binding, antigen binding, carbohydrate binding, G-protein coupled chemoattractant receptor activity, and chemokine receptor activity. Our results confirm previous reports describing the critical role of immune cells and ECM molecules in the construction of the TME and the relationship between this microenvironment and SKCM progression[17, 18]. We also studied the role of DEG in the prognosis of SKCM and identified 15 genes related to the TME. The expression of *TLR7*, *AQP9*, *CCR8*, *PATL2*, *RGL4*, *OR9G1*, *CXCR5*, *IPCEF1*, *FCRL3*, *RCSL1*, *CP*, *NEXN*, *MAFB*, *SLC40A1*, and *TNFRSF13B* is related to the survival of patients with SKCM.

We elucidated the interactions between DEGs by constructing a PPI network and discovered that all important genes are involved in the immune/inflammatory response. The top 20 important genes were *CD72*, *CXCR3*, *CCR8*, *CXCL13*, *C1R*, *C1S*, *CXCL9*, *CXCL16*, *CCL25*, *CXCR5*, *CXCL10*, *CCR2*, *CD8B*, *CXCL11*, *CCR7*, *C1QC*, *CD3G*, *CCL21*, *HLA-DRB5*, and *CCL19*. These genes have been reported to be involved in cell proliferation, apoptosis, angiogenesis, migration, and immune responses[19, 20].

Next, we selected *CCR8* and *CXCR5* as key genes by combining significant DEGs and prognosis-associated genes. Loss of *CXCR4*, *CXCR5*, and *CCR9* in circulating T-cell subsets has been reported to be associated with pulmonary involvement[21]. As a skin homing receptor, *CCR8* is expressed in most T cells in normal skin and produces proinflammatory cytokines[22]. We then used the LinkedOmics database to explore kinase targets for the *CCR8* and *CXCR5* hubs. *PRKCA*, *ATM*, *PLK1*, *CHEK1*, and *ATR* are the five most significant kinase targets of *CXCR5*. Kinases *LYN*, *FYN*, *AURKB*, *PAK1*, and *LCK* are the five most prominent target networks for *CCR8*. We continued to study the coexpression genes of the *CCR8* and *CXCR5*. Studies have shown that *MAPK1* and other kinase targets can regulate the cell cycle, epithelial–mesenchymal transformation, and tumor cell invasion and metastasis[23]. The results also suggest that *CCR8* and *CXCR5* may regulate the cell cycle, epithelial–mesenchymal transformation, and tumor cell invasion and metastasis of SKCM. Increasing evidence of a significant association between immune cell infiltration and patient prognosis in many tumor types has been reported[24].

Finally, we investigated the immune cell infiltration of *CCR8* and *CXCR5*. The results showed that *CCR8* and *CXCR5* are positively correlated with the infiltration of neutrophils, macrophages, and CD8+ T, CD4+ T, B, and dendritic cells. Studies have shown that enhanced CD8+T-cell trafficking is very important in the anti-PD-1/anti-CTLA-4 efficacy of melanoma brain metastases, which may be an immunotherapeutic enhancement strategy[25]. The interaction between melanoma and immune cells has also been studied, and the key role of these cells in tumor growth and the immune response has been emphasized[26]. Thus, these genes may provide additional information on the correlation between immune cell infiltration and clinical outcomes in SKCM patients.

The TME is involved in the development of cancer and interacts with SKCM, thus affecting the progression, metastasis, drug resistance, and prognosis of the disease. This study evaluated the

relationship between the immune/stromal scores and clinical characteristics of patients with SKCM. The function and prognostic value of TME-related genes were also investigated. Our findings add to the existing body of knowledge on the complex interactions between SKCM and its tumor environment. However, the results of our study are very limited because it was carried out in a small population. Therefore, a more comprehensive analysis of a larger corpus of patient data is necessary to reveal the complex relationship between SKCM and its TME.

5. Conclusions

In summary, we evaluated the immune score and stromal score of SKCM by using the ESTIMATE algorithm, and studied the genes related to the tumor microenvironment by functional enrichment analysis. Our study provides new biomarkers for the treatment and prognosis of SKCM.

6. Declarations

6.1 Ethics approval and consent to participate

The data in this study are from public databases on the Internet and do not involve ethical issues.

6.2 Consent for publication

All authors read and approved the final manuscript.

6.3 Availability of data and materials

The data of this study includes two aspects. Protein data can be downloaded from the TCPA database (<https://www.tcpaportal.org>), while clinicopathological data can be downloaded from the TCGA database (<https://www.tcpaportal.org/tcpa/>).

6.4 Competing interests

The authors declare that there are no conflict of interests.

6.5 Funding

This work was supported by High-level Hospital Construction Research Project of Maoming People's Hospital, Medical Science and Technology Research Foundation of Guangdong Province (Project No.: B2020194), China Postdoctoral Foundation (Project No.:2018m633286).

6.6 Authors' contributions

Guangwen Wang and Yonghuo Ling have contributed equally to this work.

6.7 Acknowledgements

The authors would like to thank those involved in Department of Dermatology, Department of Oncology and Center of Scientific Research for their valuable support and helpful discussions.

7. References

1. Fischer GM, Gopal YNV, McQuade JL, Peng W, DeBerardinis RJ, Davies MA: Metabolic strategies of melanoma cells: Mechanisms, interactions with the tumor microenvironment, and therapeutic implications. *PIGM CELL MELANOMA R* 2018, 31(1):11-30.
2. Aubuchon MMF, Bolt LJJ, Janssen-Heijnen MLG, Verleisdonk-Bolhaar STHP, van Marion A, van Berlo CLH: Epidemiology, management and survival outcomes of primary cutaneous melanoma: a ten-year overview. *ACTA CHIR BELG* 2017, 117(1):29-35.
3. Veierød MB: Melanoma incidence on the rise again. *Tidsskrift for den Norske laegeforening : tidsskrift for praktisk medicin, ny raekke* 2015, 135(5):450-452.
4. Gajewski TF, Schreiber H, Fu Y: Innate and adaptive immune cells in the tumor microenvironment. *NAT IMMUNOL* 2013, 14(10):1014-1022.
5. Di Jia, Li S, Li D, Xue H, Yang D, Liu Y: Mining TCGA database for genes of prognostic value in glioblastoma microenvironment. *Aging* 2018, 10(4):592-605.
6. Hui L, Chen Y: Tumor microenvironment: Sanctuary of the devil. *CANCER LETT* 2015, 368(1):7-13.
7. Romero-Garcia S, Moreno-Altamirano MMB, Prado-Garcia H, Sánchez-García FJ: Lactate Contribution to the Tumor Microenvironment: Mechanisms, Effects on Immune Cells and Therapeutic Relevance. *FRONT IMMUNOL* 2016, 7:52.
8. Lambrechts D, Wauters E, Boeckx B, Aibar S, Nittner D, Burton O, Bassez A, Decaluwé H, Pircher A, Van den Eynde K et al: Phenotype molding of stromal cells in the lung tumor microenvironment. *NAT MED* 2018, 24(8):1277-1289.
9. Yoshihara K, Shahmoradgoli M, Martínez E, Vegesna R, Kim H, Torres-García W, Treviño V, Shen H, Laird PW, Levine DA et al: Inferring tumour purity and stromal and immune cell admixture from expression data. *NAT COMMUN* 2013, 4:2612.
10. Vincent KM, Findlay SD, Postovit LM: Assessing breast cancer cell lines as tumour models by comparison of mRNA expression profiles. *Breast cancer research : BCR* 2015, 17:114.
11. Shah N, Wang P, Wongvipat J, Karthaus WR, Abida W, Armenia J, Rockowitz S, Drier Y, Bernstein BE, Long HW et al: Regulation of the glucocorticoid receptor via a BET-dependent enhancer drives antiandrogen resistance in prostate cancer. *ELIFE* 2017, 6.
12. Alonso MH, Aussó S, Lopez-Doriga A, Cordero D, Guinó E, Solé X, Barenys M, de Oca J, Capella G, Salazar R et al: Comprehensive analysis of copy number aberrations in microsatellite stable colon cancer in view of stromal component. *BRIT J CANCER* 2017, 117(3):421-431.
13. Tomczak K, Czerwińska P, Wiznerowicz M: The Cancer Genome Atlas (TCGA): an immeasurable source of knowledge. *Contemporary oncology (Poznan, Poland)* 2015, 19(1A):68-77.

14. Li T, Fan J, Wang B, Traugh N, Chen Q, Liu JS, Li B, Liu XS: TIMER: A Web Server for Comprehensive Analysis of Tumor-Infiltrating Immune Cells. *CANCER RES* 2017, 77(21):108-110.
15. Szklarczyk D, Gable AL, Lyon D, Junge A, Wyder S, Huerta-Cepas J, Simonovic M, Doncheva NT, Morris JH, Bork P et al: STRING v11: protein-protein association networks with increased coverage, supporting functional discovery in genome-wide experimental datasets. *NUCLEIC ACIDS RES* 2019, 47:607-613.
16. Vasaikar SV, Straub P, Wang J, Zhang B: LinkedOmics: analyzing multi-omics data within and across 32 cancer types. *NUCLEIC ACIDS RES* 2018, 46:956-963.
17. Marzagalli M, Ebelt ND, Manuel ER: Unraveling the crosstalk between melanoma and immune cells in the tumor microenvironment. *SEMIN CANCER BIOL* 2019, 59:236-250.
18. Forsthuber A, Lipp K, Andersen L, Ebersberger S, Graña-Castro O, Ellmeier W, Petzelbauer P, Lichtenberger BM, Loewe R: CXCL5 as Regulator of Neutrophil Function in Cutaneous Melanoma. *The Journal of investigative dermatology* 2019, 139(1):186-194.
19. F A, J L, S K, SC G, Le Naour R, JM S, W H, F G, P B: CXCL10 reduces melanoma proliferation and invasiveness in vitro and in vivo. *The British journal of dermatology* 2011, 164(4):720-728.
20. Roberts EW, Broz ML, Binnewies M, Headley MB, Nelson AE, Wolf DM, Kaisho T, Bogunovic D, Bhardwaj N, Krummel MF: Critical Role for CD103(+)/CD141(+) Dendritic Cells Bearing CCR7 for Tumor Antigen Trafficking and Priming of T Cell Immunity in Melanoma. *CANCER CELL* 2016, 30(2):324-336.
21. Jacquelot N, Enot DP, Flament C, Vimond N, Blattner C, Pitt JM, Yamazaki T, Roberti MP, Daillère R, Vétizou M et al: Chemokine receptor patterns in lymphocytes mirror metastatic spreading in melanoma. *The Journal of clinical investigation* 2016, 126(3):921-937.
22. Klarquist J, Denman CJ, Hernandez C, Wainwright DA, Strickland FM, Overbeck A, Mehrotra S, Nishimura MI, Le Poole IC: Reduced skin homing by functional Treg in vitiligo. *Pigment Cell Melanoma Res* 2010, 23(2):276-286.
23. Li XW, Tuergan M, Abulizi G: Expression of MAPK1 in cervical cancer and effect of MAPK1 gene silencing on epithelial-mesenchymal transition, invasion and metastasis. *ASIAN PAC J TROP MED* 2015, 8(11):937-943.
24. Y I, R Y, K S, M I, T K, Y K, N H: Immune cell infiltration as an indicator of the immune microenvironment of pancreatic cancer. *BRIT J CANCER* 2013, 108(4):914-923.
25. Taggart D, Andreou T, Scott KJ, Williams J, Rippaus N, Brownlie RJ, Ilett EJ, Salmond RJ, Melcher A, Loriger M: Anti-PD-1/anti-CTLA-4 efficacy in melanoma brain metastases depends on extracranial disease and augmentation of CD8 T cell trafficking. *P NATL ACAD SCI USA* 2018, 115(7):1540-1549.
26. Hölzel M, Tüting T: Inflammation-Induced Plasticity in Melanoma Therapy and Metastasis. *TRENDS IMMUNOL* 2016, 37(6):364-374.

Tables

Table 1: The kinase target networks of CXCR5 and CCR8 in SKCM (LinkedOmics).

	Gene Set	Description	Leading Edge Number	P Value
CXCR5	Kinase_PRKCA	protein kinase C alpha	68	0
	Kinase_ATM	ATM serine/threonine kinase	58	0
	Kinase_PLK1	polo like kinase 1	44	0
	Kinase_CHEK1	checkpoint kinase 1	43	0
	Kinase_ATR	ATR serine/threonine kinase	28	0.045455
CCR8	Kinase_FYN	FYN proto-oncogene, Src family tyrosine kinase	24	0
	Kinase_LYN	LYN proto-oncogene, Src family tyrosine kinase	24	0
	Kinase_AURKB	aurora kinase B	24	0
	Kinase_PAK1	p21 (RAC1) activated kinase 1	23	0
	Kinase_LCK	LCK proto-oncogene, Src family tyrosine kinase	20	0

Figures

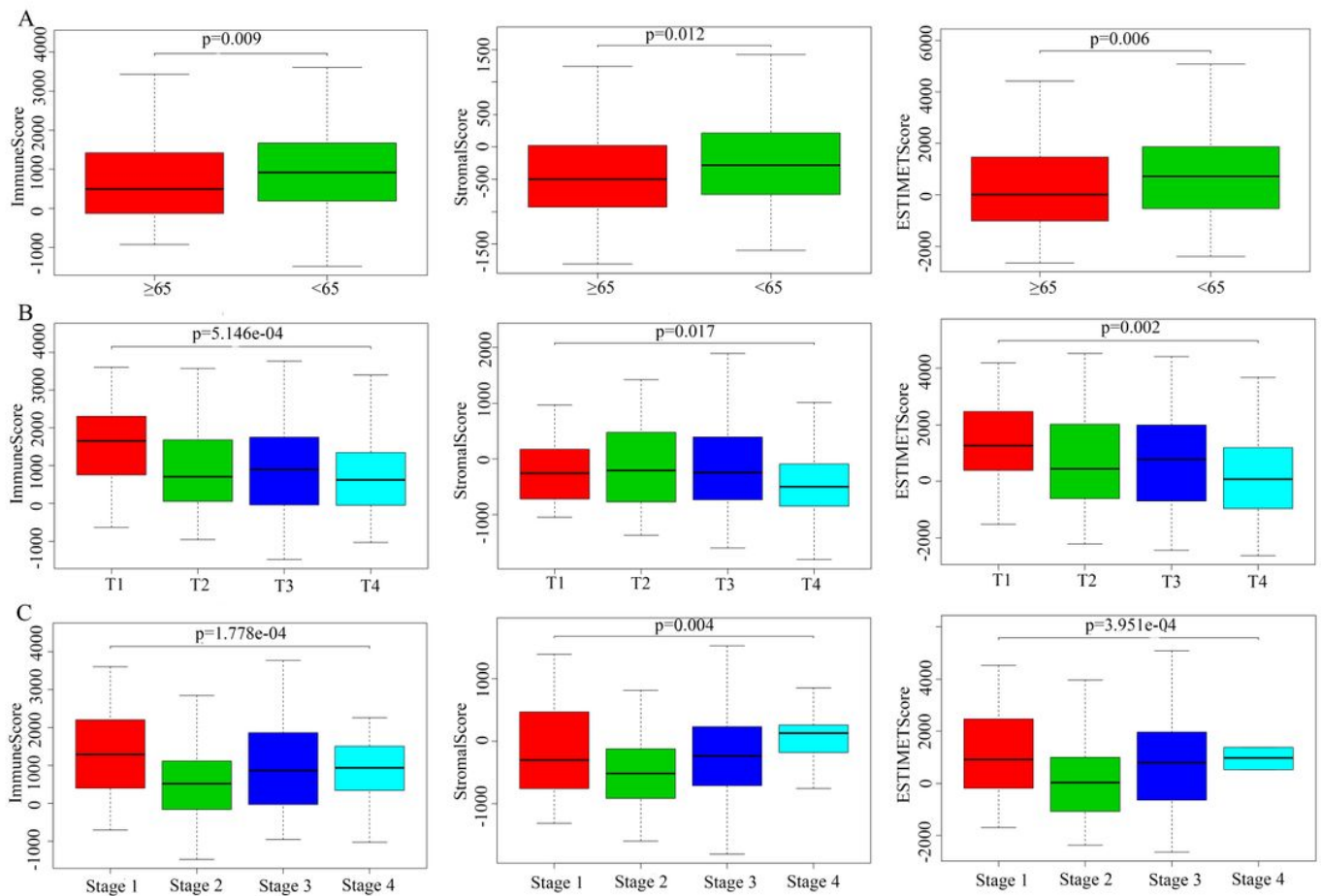


Figure 1

Association between immune/stromal scores and clinicopathologic variables in SKCM. (A) A significant association was revealed between age and the level of immune scores ($P = 0.009$) \times stromal scores ($P = 0.012$), and ESTIMATE score ($P = 0.006$). (B) A significant association was revealed between T stage and the level of immune scores ($P = 5.146 \times 10^{-4}$) \times stromal scores ($P = 0.017$), and ESTIMATE score ($P = 0.002$). (C) A significant association was revealed between tumor stage and the level of immune scores ($P = 1.778 \times 10^{-4}$) \times stromal scores ($P = 0.004$), and ESTIMATE score ($P = 3.951 \times 10^{-4}$).

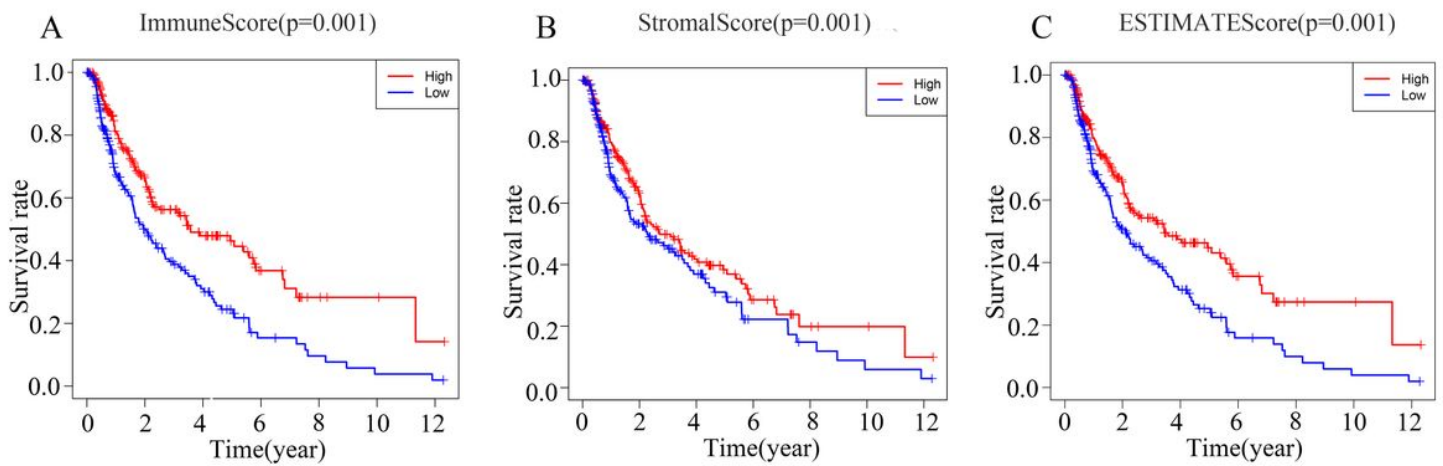


Figure 2

Association between immune/stromal scores and overall survival in SKCM. (A) Overall survival in SKCM patients with high immune scores is poorer than of patients with low immune scores ($P = 0.001$). (B) Overall survival in SKCM patients with high stromal scores is poorer than that of patients with low stromal immune scores ($P = 0.069$). (C) Overall survival in SKCM patients with high ESTIMATE score is poorer than that of patients with low ESTIMATE scores ($P = 0.001$). The logrank test was used to calculate the P-value.

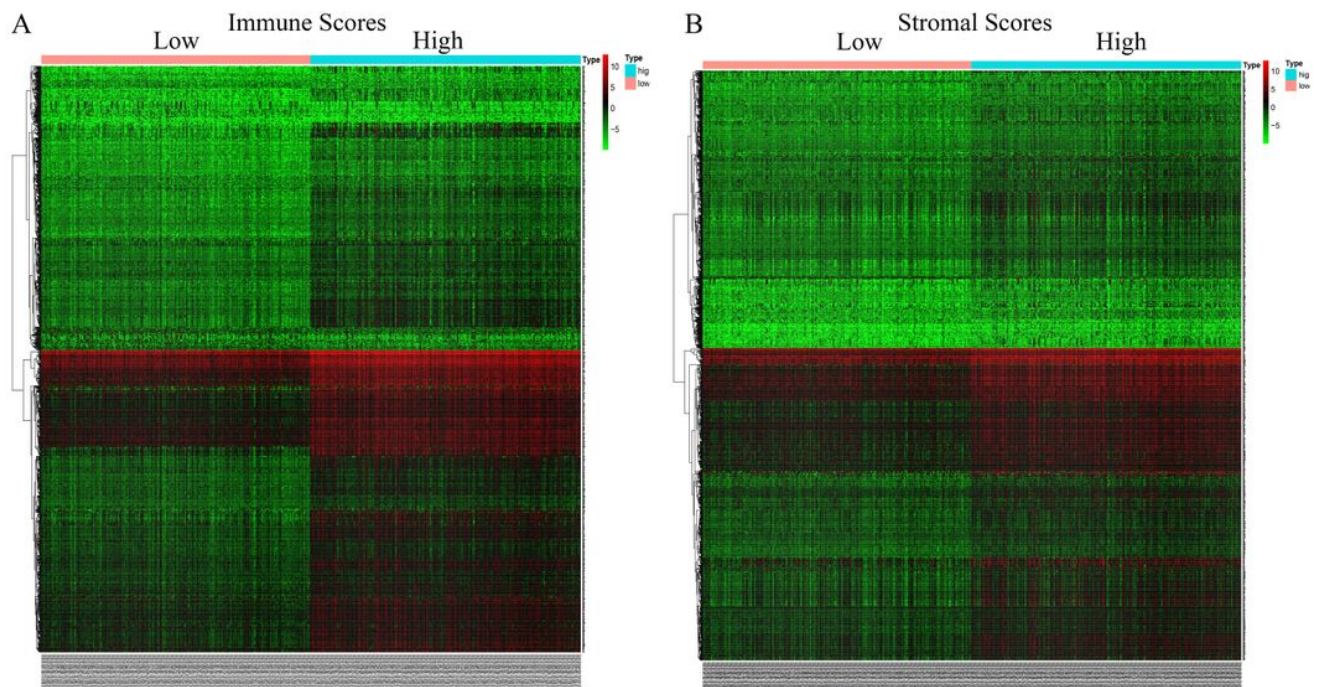


Figure 3

Comparison between the gene expression profiles and immune/stromal scores in SKCM. (A) Heatmap of the DEGs in immune scores comparing high score and low score groups ($P < 0.05$, $|\text{fold change}| > 2$). (B) Heatmap of the DEGs in stromal scores comparing high score and low score groups ($p < 0.05$, $|\text{fold change}| > 2$).

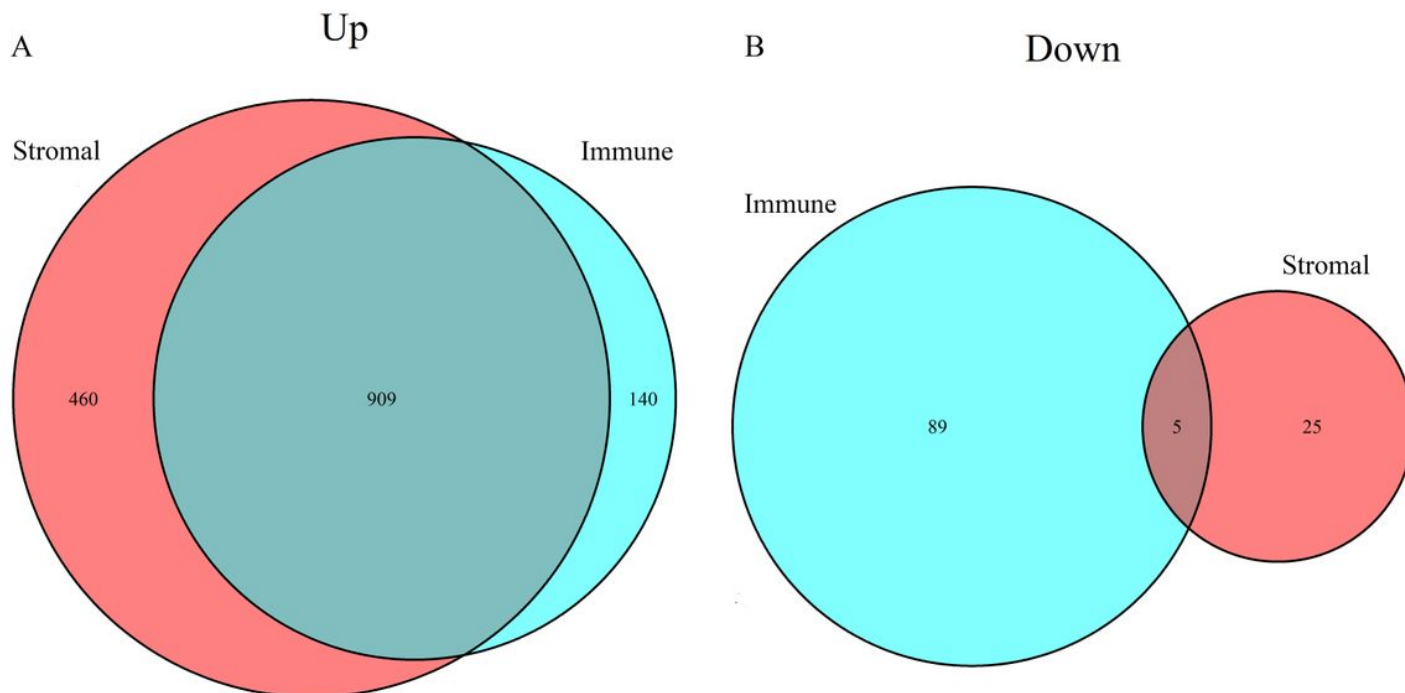


Figure 4

The number of upregulated genes (A) or downregulated genes (B) DEGs in stromal and immune score groups in Venn diagrams. Venn diagram analysis of aberrantly expressed genes based on immune and stromal scores.

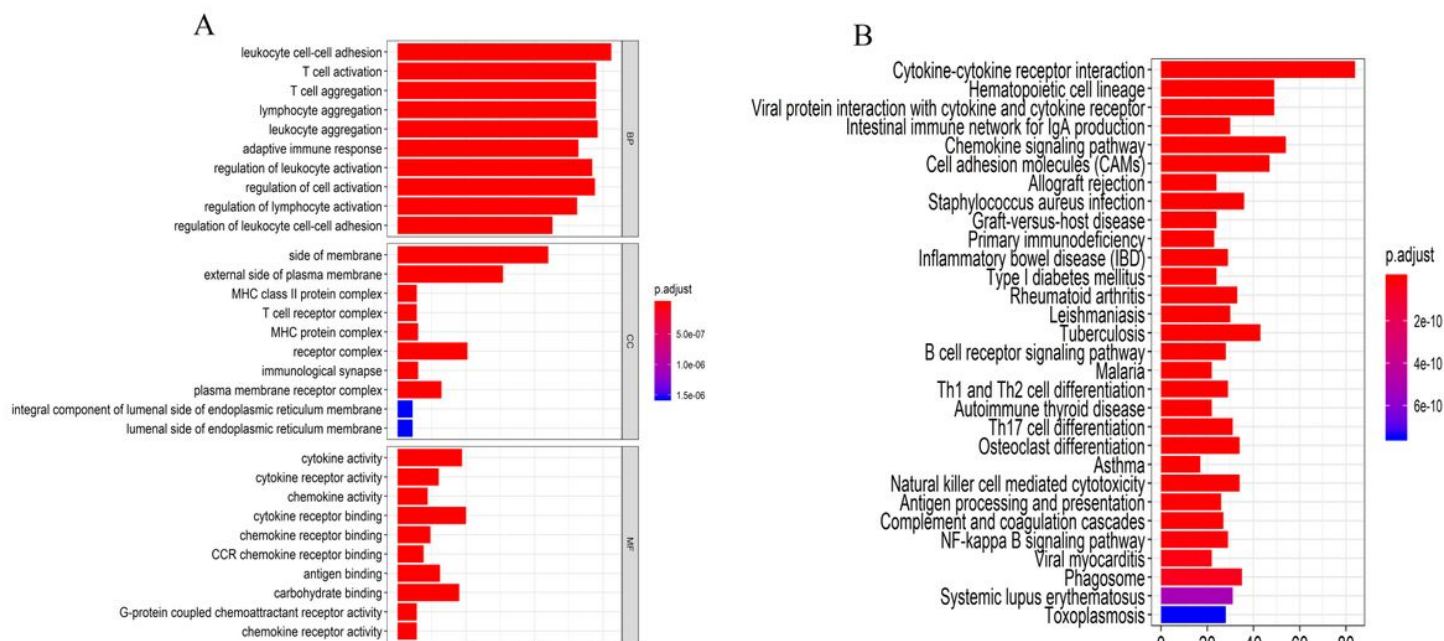


Figure 5

Functional enrichment analysis of DEGs. (A) Top 10 terms in GO analysis with $P < 0.05$. (B) The enriched terms in KEGG pathways analysis $p < 0.05$.

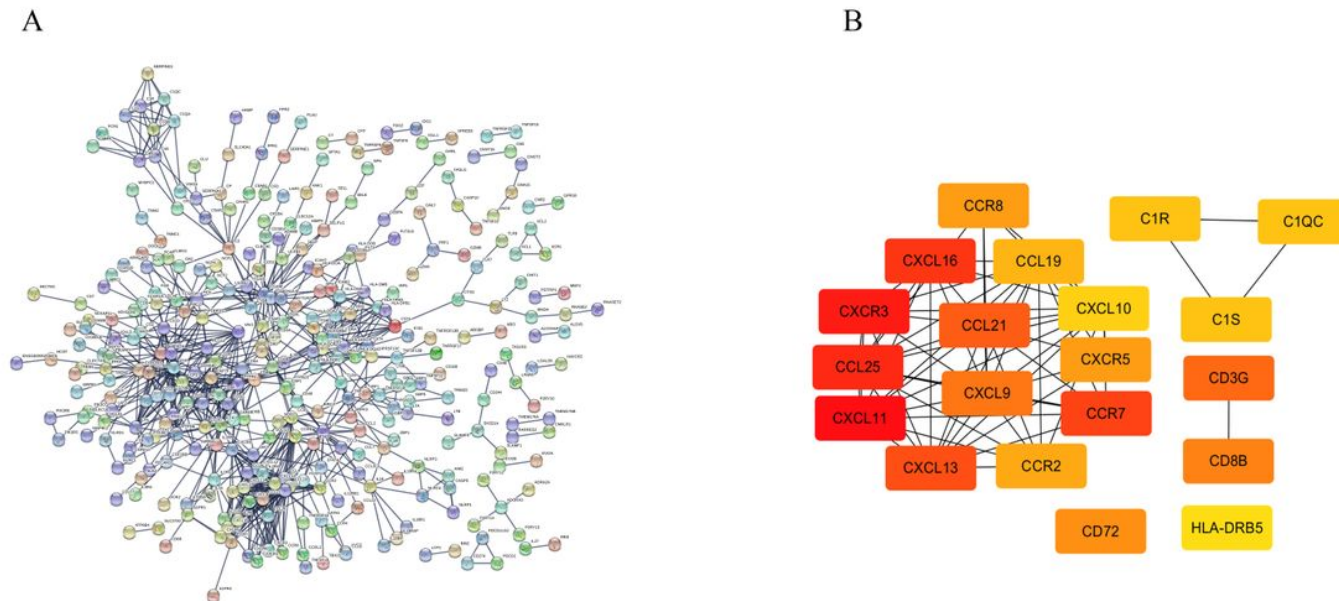


Figure 6

Commonly DEGs PPI networks constructed by STRING tool and Cytoscape. (A) There were a total of 162 DEGs in the PPI network complex. The nodes meant genes; the edges meant the interaction of genes; (B) The significant genes in PPI networks via CytoHubba plug-in (degree cutoff = 2, node score cutoff = 0.2, k-core = 2, and max. Depth = 100).

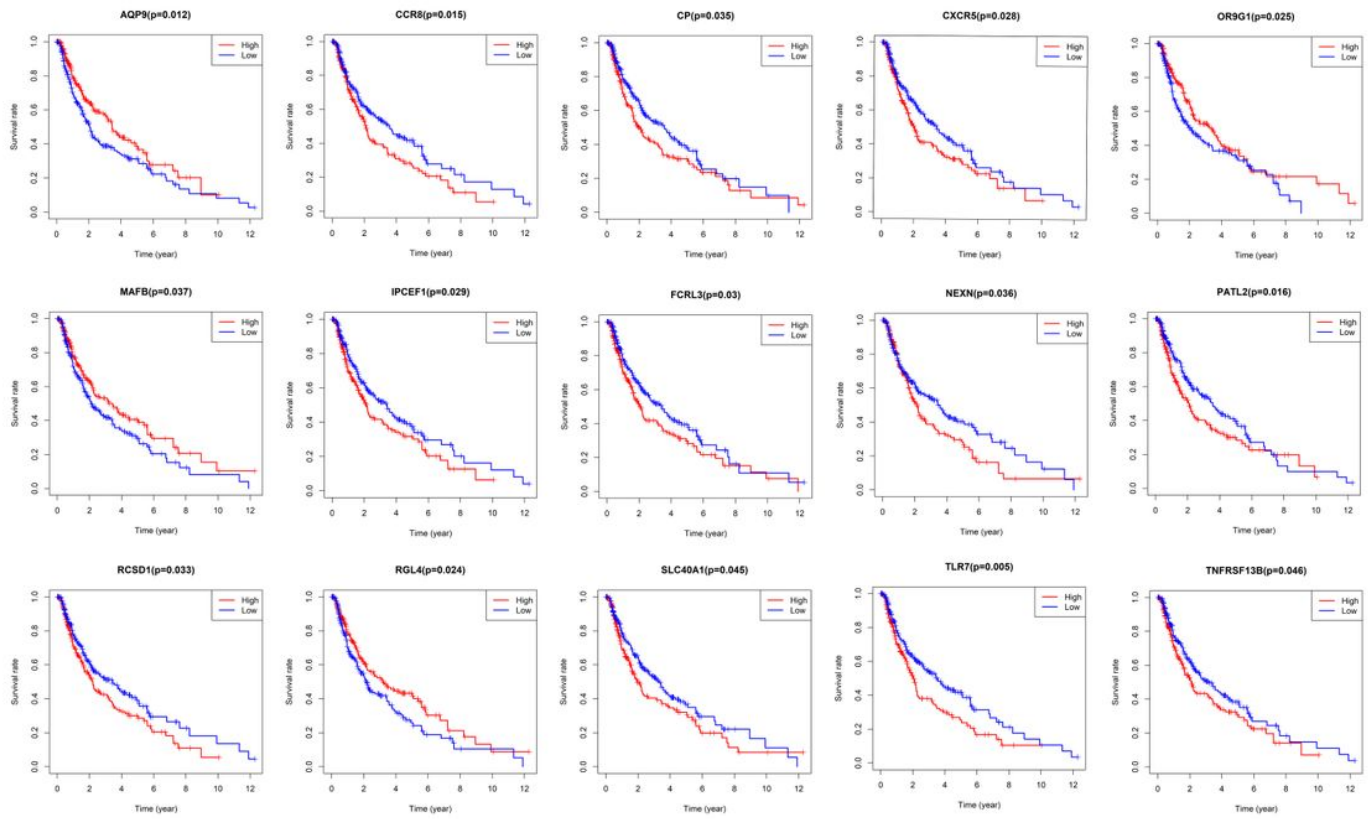


Figure 7

The Kaplan–Meier survival curves for 15 genes (TLR7, AQP9, CCR8, PATL2, RGL4, OR9G1, CXCR5, IPCEF1, FCRL3, RCSD1, CP, NEXN, MAFB, SLC40A1, TNFRSF13B) associated with overall survival. Horizontal axis: overall survival time, years; Vertical axis: survival function.

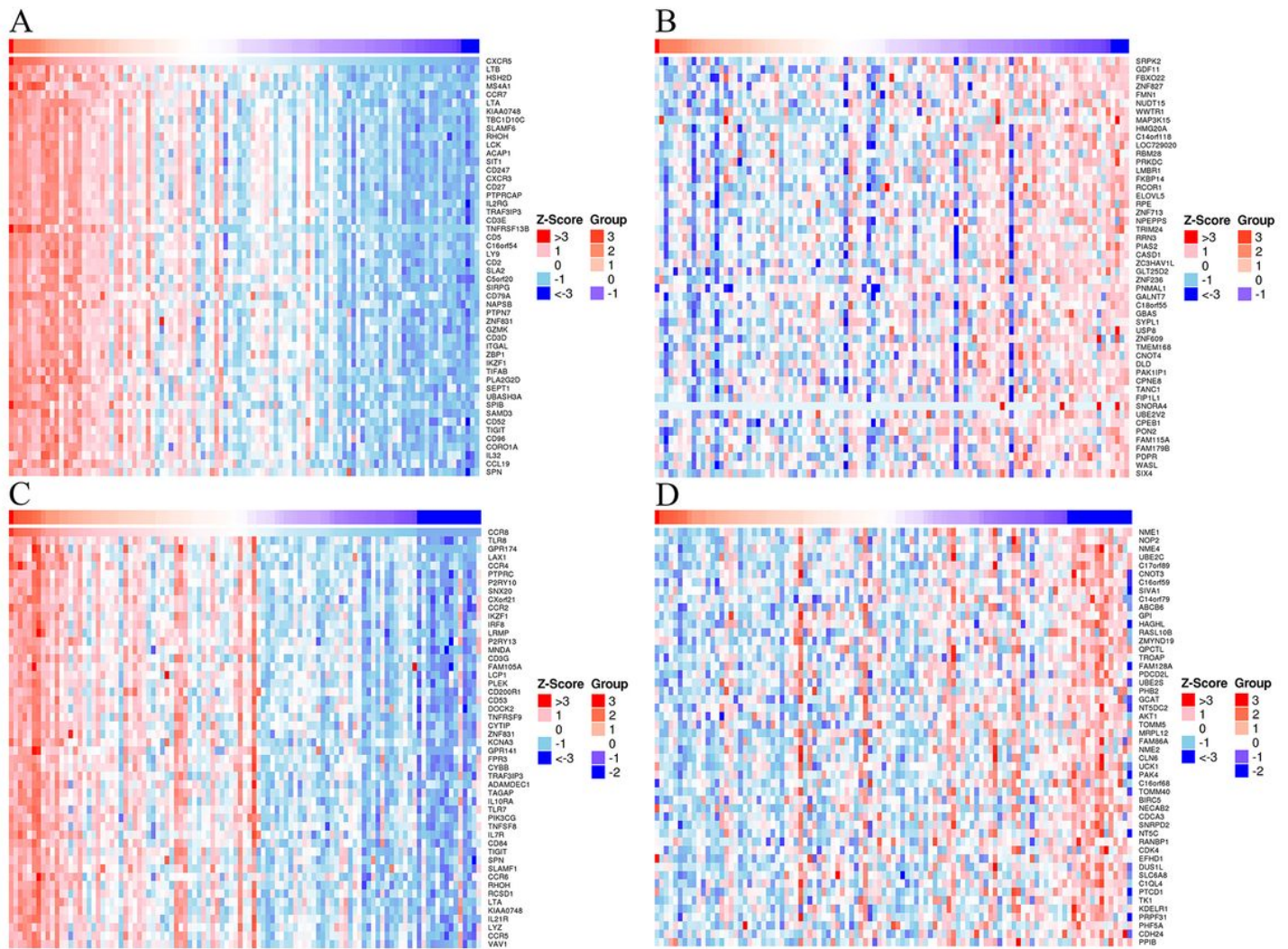


Figure 8

The positively correlated significant genes (A) and the negatively correlated significant genes (B) of CXCR5; The positively correlated significant genes (C) and the negatively correlated significant genes (D) of CCR8.

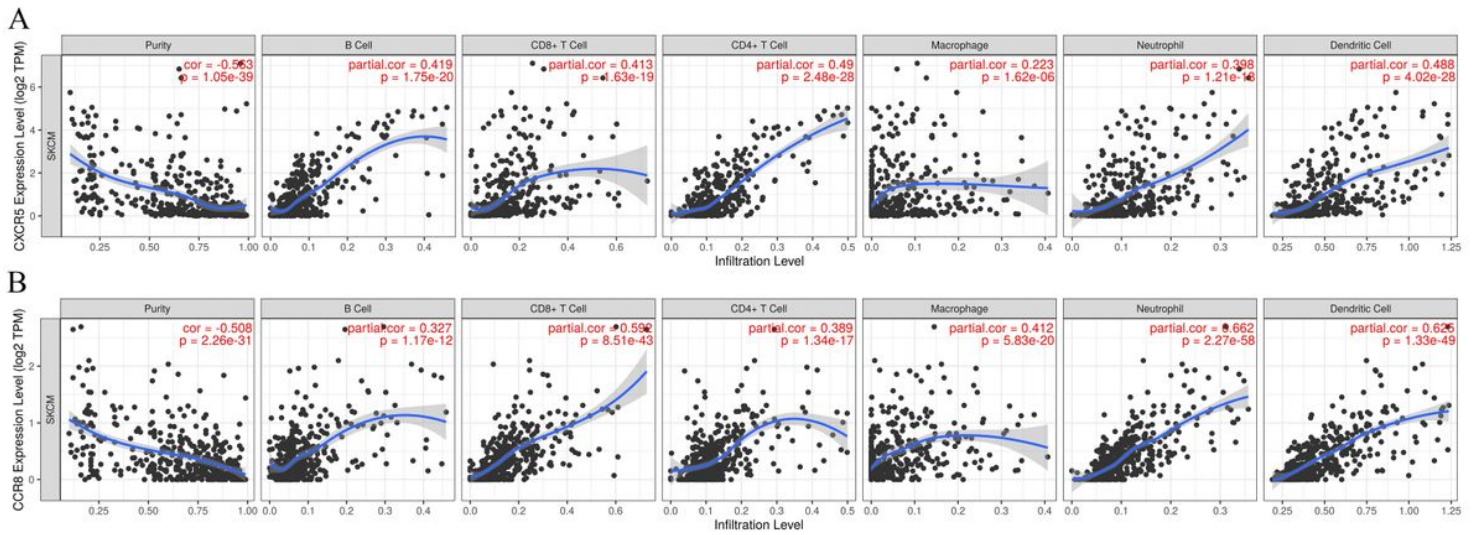


Figure 9

The correlation between hub genes and immune cell infiltration (A for CXCR5; B for CCR8).